Effect of Moving Load on the Deformation of Asphalt Pavement

N. Abe
Toa Road Corporation, Minato ward, TOKYO, Japan

J, Mizukami
National Institute for Land and Infrastructure Management, Yokosuka, KANAGAWA, Japan

M, Kimura
Tokyo Sokki Kenkyujo Co., Ltd., Shinagawa ward, TOKYO, Japan

ABSTRACT: To examine the behavior of asphalt pavement affected by temperature change during construction or changes in air temperature, two types of strain gauge were embedded in the asphalt pavement. KM strain gauges and fiber-optic FBG sensors were set under the binder course, under the asphalt-stabilized layer and on the subgrade surface. In addition, changes in strain in the pavement were examined under applied load from a moving aircraft and FWD test. The largest amplitude of strain vibration induced by applied moving load was measured under the asphalt-stabilized base layer. From the result, it is assumed that the failure criterion of the asphalt-stabilized base layer has an overall effect on the pavement. The strain corrugation that occurs under the asphalt mixture shows two piles due to the moving load, but the one on the top of the subgrade shows one pile and longer loading time. In conventional pavement design, the established standard is at the surface of the subgrade under the center of the load, and the validity of the design method was confirmed. The strains across and along the runway that were measured during applied load on a circular plate were similar to each other, showing that the elasticity theory can be used to analyze pavement structures.
The calculated and measured strains were very similar at the underside of the stabilized base directly under the moving wheels. On the other hand, the calculated strain values at the bottom of the stabilized base and at the top of the subgrade under the gear center were considerably smaller than the strain values measured with KM strain gauges. Dynamic analysis will be conducted by also considering movement along the gear moving direction.
From the above, the structural evaluation of asphalt pavement requires an approach that takes into consideration the loading time.

KEY WORDS: Moving load, FWD, FBG sensor, strain gauge, dynamic analysis.

1 INTRODUCTION

When load is applied to pavement, the pavement deforms downward, and stress and strain are generated in the pavement. Repetitive application of load by landing aircraft causes lingering strain and the accumulation of residual deformation, which leads to fatigue cracking, settlement and destruction of the pavement. Thus, runway pavement must be monitored for internal stress and strain. Structural and design analysis is also essential.
To understand the deformation behavior of asphalt concrete pavement under the load of aircraft landing gear, KM strain gauges and fiber-optic FBR strain sensors were installed

under the binder course, at the bottom of the stabilized base, and at the top of the subgrade. Under today's standards, the destruction of asphalt concrete pavement is examined based on the bending tensile strain at the underside of the asphalt concrete mixture and the compressive strain at the top of the subgrade.

This paper describes the strain in pavement generated by moving load (aircraft landing gear) and the falling weight deflectometer (FWD) test, which measures the deflection of the pavement at the time of impact, and compares the results of static and dynamic structural analyses. The results were used to examine the validity of structural analysis and theoretical design methods.

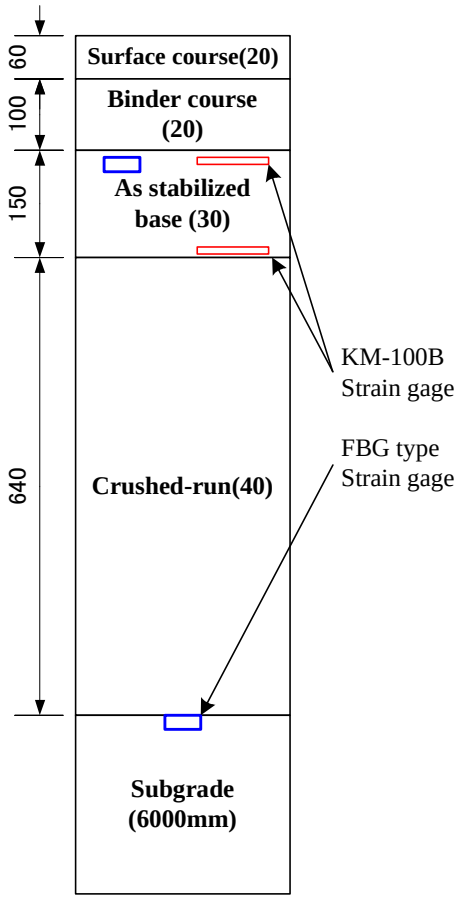

Figure 1 Pavement structure of runway (LA-1)

2 PAVEMENT STRUCTURE AND EMBEDDED DEVICES

2.1 Pavement structure

The runways of major airports have the pavement structure shown in Figure 1. This structure, which is classified as LA-1, is designed to resist 20,000 repetitive load applications by a Boeing 747, which is the representative aircraft.

The surface course consists of a dense-grade asphalt concrete mixture with a maximum aggregate size of 20 mm. The design depth is 60 mm to allow grooving. In this study, 150 mm of pavement was cut and overlaid after 10,000 passes of a moving load in order to check the fatigue resistance of asphalt stabilization.

In the moving load test, the load was set to 910 kN to reproduce the design gear load of a Boeing 747 and the maximum moving speed was set to 5 km/h. The installation width and contact pressure of the tires were set to the values listed in Reference 1.

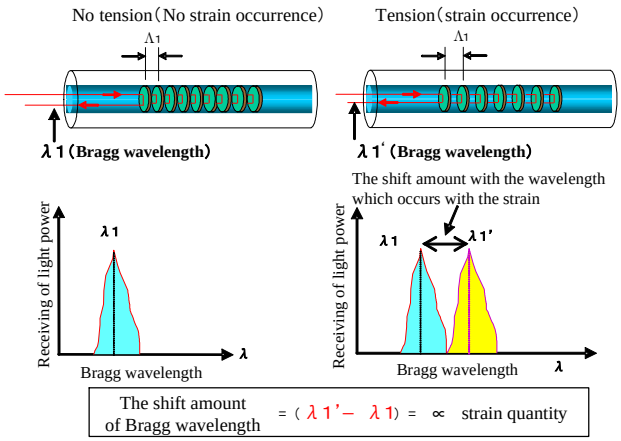

Figure 2 The principle of the FBG type optical fiber sensor

2.2 Embedded devices

2.2.1 Concept and installation of FBG strain sensors

A fiber Bragg grating (FBG) uses optical fibers as measuring sensors. Unlike conventional electric systems, in which measuring sensors are connected to cables for transmitting signals, FBR measures and transmits signals using a single optical fiber. As shown in Figure 2,

sections (gratings) that differ in refraction are arranged like gratings in the middle of an optical fiber and are used as a sensor (FBG sensor).

The gratings are arranged at a high density of 20,000 within a length of 10 mm. Incident light from one end passes through the optical fiber, and only specific wavelengths (Bragg wavelengths) are reflected at the FBG sensor and returned.

The Bragg wavelength changes depending on the width of the gratings at the sensor. Strain change of 1 μm at the gratings is known to cause a 1.2-pm change in Bragg wavelength. This principle is used in FBG to measure strain. Fibers can be as long as 30 km, and the system is capable of measuring compressive strain as well as tensile strain.

To measure horizontal strain, gauges were installed at the upperside of the subgrade (Photo 1) and at the underside of the stabilized base.

Using FBG sensors that were installed during construction of the pavement, we measured the dynamic strain during applied moving loads and the static strain during no load.

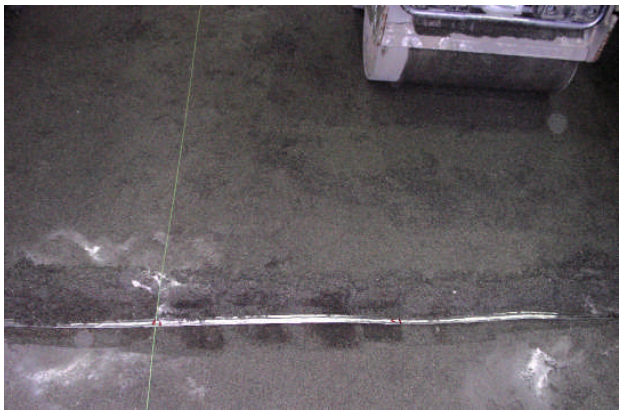

Photo 1 The establishment status to the top surface of the subgrade with FBG type strain gauge

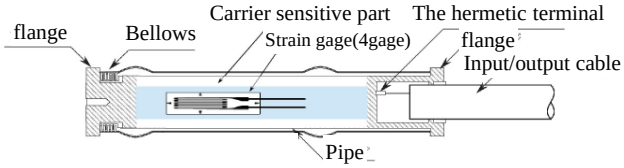

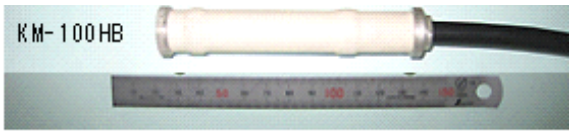

Figure 3 The structure and the size with KM type ground-coupled strain gauge

2.2.2 Concept and installation of KM strain gauges

In this study, strain gauges for monitoring the deformation of asphalt concrete pavement were installed at the top and undersides of the stabilized base both across and along the runway to prevent any damage from cutting and overlaying after 10,000 passes of a moving load.

Photo 2 The overview of this moving load equipment

The KM strain gauges had to be heat resistant and durable due to exposure to temperatures exceeding 100°C during the spreading of the asphalt concrete mixture, and vibration during roll compaction. Based on the results of a comparative test of strain gauges (Reference 2), KM-100HB (Tokyo Sokki Kenkyujo Co. Ltd.) was selected for use.

The structure of this KM strain gauge is shown in Figure 3. It provides high insulation performance and so can be used in a moist environment. The apparent modulus of elasticity is rather low at 40 N/mm^2, and the internal structure is designed to eliminate the bending component of the strain. As the size of strain gauges should be at least 3 times larger than the maximum aggregate size, the KM gauge was judged appropriate for this experiment.

3 TEST RESULTS

3.1 Loading conditions of moving load test

The loading equipment shown in Photo 2 was used to apply moving load equivalent to the gear load of a Boeing 747 on the pavement installed with sensors.
The equipment included a computer system for controlling the load, traveling speed, and other test conditions and a hydraulic system for applying and controlling the moving load.
In this experiment, the position of applied load and the number of passes were decided and set in advance. The contact pressure from the aircraft wheels and the strain at the surface of the pavement generated by the wheels were reported in our previous paper (Reference 2). The relationship between the moving speed of the gear load and the actual load applied is shown in Figure 4.
At instants when the vertical movement of the landing gear reversed, the moving speed of the gear decelerated and the load dropped. The gear showed vertical movement of 200 mm while moving due to the action of the damper at the center of the gear.

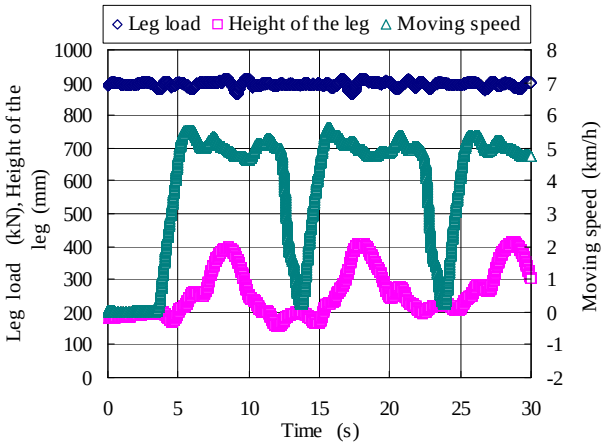

Figure 4 The Relationship between the actual gear load and the moving speed

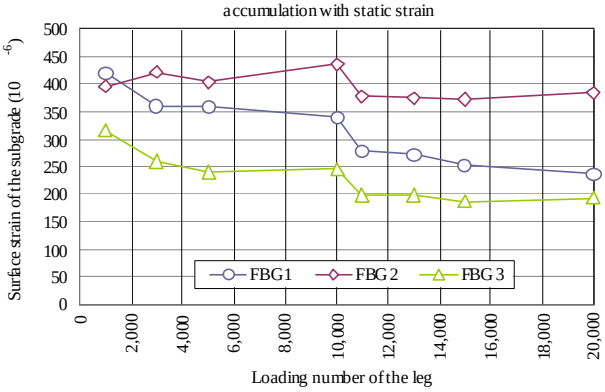

Figure 5 The change of the static strain of the subgrade to the loading number of the gear

3.2 Changes in static strain

The FBG sensors on the surface of the subgrade were installed between thin plates to detect horizontal tensile strain while canceling bending strain. Changes in static strain at the upperside of the subgrade accompanying an increase in the number of gear load passes are shown in Figure 5. In the Figure ure, FBG1 and FBG3 were directly under the wheels, and FBG2 was under the center of the gear. As the number of passes increased, the static strain decreased, and rutting of the runway pavement progressed. The FBG sensors installed at the subgrade (950 mm under the pavement) showed an increase in bending strain due to the moving load compressing the pavement.
After the pavement was cut and overlaid after 10,000 passes, changes in static strain were small. This was likely due to the subgrade and subbase course becoming increasingly compacted by repetitive load application and thus changes in static strain were not generated.
The cumulative strain at the upperside of the subgrade was largest at the gear center, which was not directly under the load. The results support the design guidelines for runway pavement, which consider the permanent deformation of subgrade as the point of destruction and require the examination of compressive strain at the upperside of the subgrade directly under the gear center. Thus, the test verified the effectiveness of calculating and checking the strain directly under the gear center.

Changes in static strain in the stabilized base from applied gear load are shown in Figure 6. As the number of applied gear loads increased, the bending of the FBG sensors increased, likely due to the development of ruts. Cutting and overlaying caused a temporary drop in cumulative strain, which started to increase again with applied gear load.

Cutting and overlaying decreased the bending strain in the pavement. The test showed that fiber-optic FBG sensors embedded in the asphalt concrete mixture and subgrade were effective for monitoring the behavior of pavement, as well as civil engineering structures.

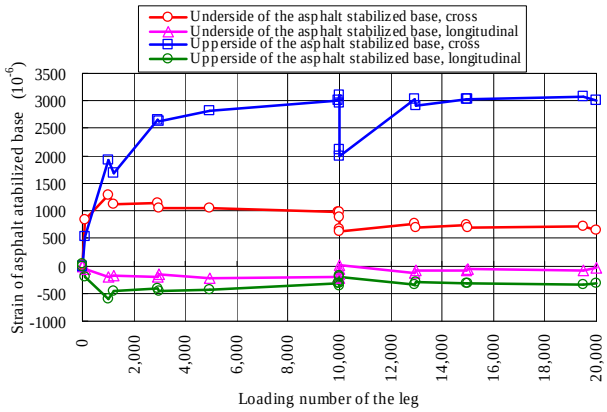

Figure 6 The change of the static strain of the upperside and the underside in the asphalt stabilized base layer to the loading number of the gear load

3.3 Strain waves during moving load test

The strain waves monitored using FBG strain gauges at the upperside of the stabilized base at the 3000th pass are shown in Figure 7. The gear load, which moved at 5 km/h, generated a similar level of tensile strain at points beneath the right and left wheels. The strain between the wheels (BWP) was compressive strain, drawing ideal strain waveforms.

The strain waves monitored using FBG sensors installed at the upperside of the subgrade at the 3000th pass are shown in Figure 8. The dynamic strain of the subgrade was tensile strain of a similar level at FBG1 and FBG2 and large tensile strain at FBG3.

Changes in the static strain were largest at FBG2, which was at the center, and smallest at FBG1, which was under the wheels. A large difference in value between FBG1 and FBG3 is likely due to the dynamic strain including the dead load of the pavement and plastic strain generated by moving loads received up to that time.

The strain waves of the stabilized base showed two peaks reflecting the distance between the front and rear wheels. The strain waves of the subgrade, which was 950 mm below the runway surface, had only one peak showing long loading time and the effects of viscoelasticity of the paving materials spread on the ground up

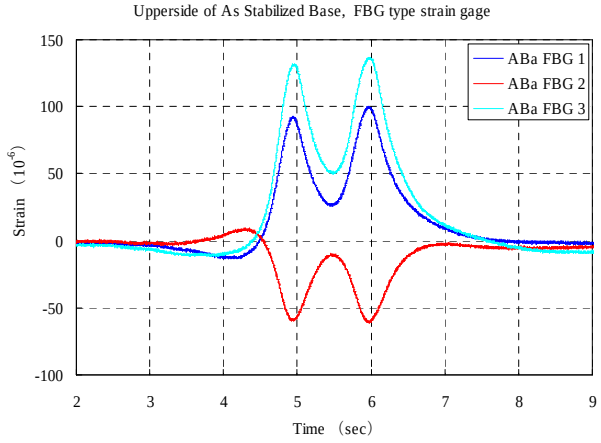

Figure 7 The strain wave which was measured with the FBG type strainmeter in the upperside of the asphalt stabilized base by the 3,000th moving load test

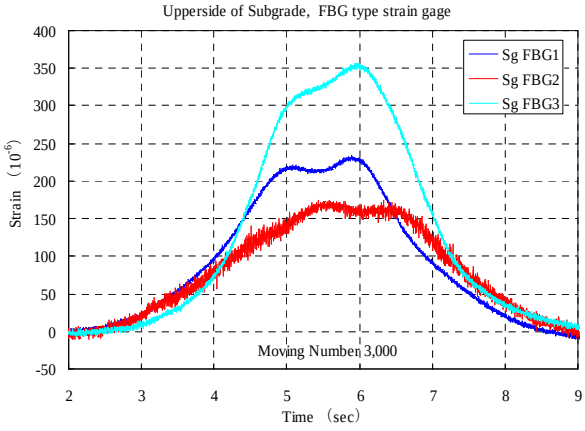

Figure 8 The strain wave by the moving load test at 3,000th with the FBG type strainmeter to have installed in the upperside of the subgrade

to the runway surface. The strain waveforms of the KM strain sensors installed across and along the runway at the bottom of the stabilized base are shown in Figure 9. The maximum strain upon the passing of a gear load was tensile strain in all KM sensors regardless of the direction of installation.

The dynamic strain at the underside of the stabilized base along the runway was compressive strain as the gear approached. The strain became tensile strain while the wheels were passing over and then changed to compressive strain after the wheels had passed.

The dynamic strain at the bottom of the stabilized base was approximately double the value at the upperside of the stabilized base. This was because the crushed-stone course beneath the stabilized base underwent significant deformation.

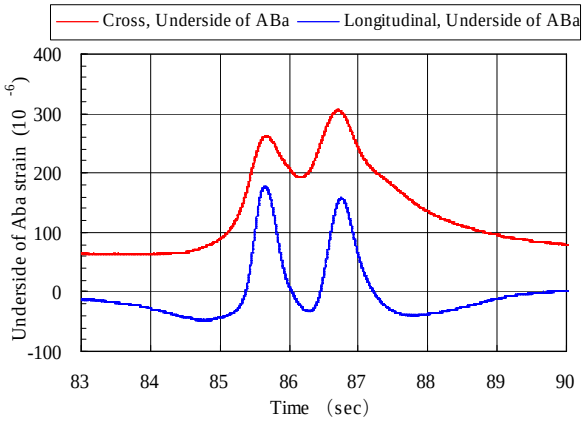

Figure 9 The strain wav with the ground-coupled strain sensor which was laid to the crossing direction and the longitude direction in the underside of the asphalt stabilized base

4 DEFLECTION MEASUREMENT USING A FALLING WEIGHT DEFLECTOMETER AND RESULTS OF ANALYSIS

4.1 Deflection curve and modulus of elasticity determined by back-calculation

The deflection caused by a load of 196 kN was measured using a Falling Weight Deflectometer (FWD) for airports on the pavement installed with strain gauges (Photo 3). Four loads were applied per point, and the mean values for the second to fourth loads were used as the representative value of the point.

Photo 3 This place implemented deflection measurement at the time of 196kN load using the FWD for the airport on the strain gauge which was laid in the pavement

The deflection curves measured for a varying number of gear load passes are shown in Figure 10. The deflection was smallest before the applied gear load and was largest after 10,000 passes. The latter was 1.7 times larger than the former, showing a reduction in pavement strength by repetitive loading.

Cutting and overlaying of pavement restored the deflection to the level at 500 passes. This was likely because the loading test had increased the residual deformation of the subgrade and the crusher run, weakened the asphalt concrete mixture and thus increased the deflection of the pavement.

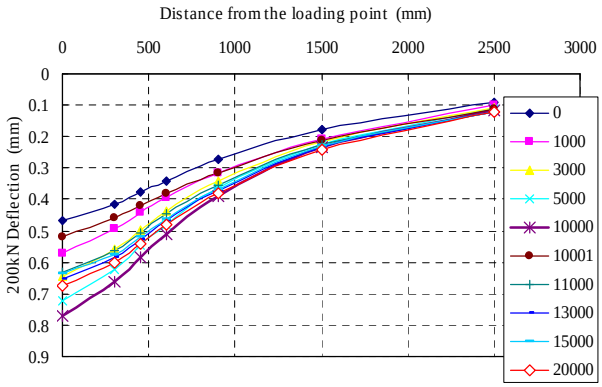

Figure 10 The deflection basin which was measured loading number of the gear

4.2 Back-calculation of modulus of elasticity and strain generated by FWD

Figure 1 shows the pavement model used to back-calculate the modulus of elasticity from the load and deflection measured using the FWD. The modulus of elasticity was calculated from the peak deflection values of the pavement structure measured with the FWD using the back-calculation program BALM (Reference 3) (developed by Prof. Kunihito Matsui, Tokyo Denki University).
The pavement model was constructed in a soil tank, and the effects of the concrete bottom 4 m from the surface were considered as the fifth and firm layer in the analysis. Based on data provided by the Service Center of Port Engineering (Reference 4), the modulus of elasticity of the firm layer was assumed to be 7,000 MPa.
The mean temperature of the asphalt concrete courses was determined from the values measured using thermocouples installed in each course using the trapezoidal rule (Reference 5). Since the rigidity of the asphalt concrete mixture changes depending on temperature, Equation (1) was used to correct the modulus of elasticity of the asphalt concrete mixture at 20°C using the measured mean temperature of the courses.
The relationship between the back-calculated modulus of elasticity and the number of gear load passes is shown in Figure 11.

$$E_{(20)} = E \times 10^{[-0.0184\times(20-T)]} \quad (1)$$

Where,
E: Modulus of elasticity of the asphalt concrete course (MPa)
E(20): Modulus of elasticity of the asphalt concrete course at 20°C (MPa)
T: Mean temperature of the asphalt concrete courses (°C)

4.3 Comparison between strain measurement during FWD test and strain values estimated by elastic analysis

Strain values of the pavement measured with the strain gauges during the FWD test were compared with the strain values obtained using the back-calculated modulus of elasticity.
The strain values at the bottom surface of the stabilized base along and across the runway, which were measured during the FWD test, are shown in Figure 12.
The dynamic strain waveforms along and across the runway, which were determined by placing the FWD loading plate on the embedded strain gauges, were mutually very similar. The results well reproduced the conformity between strains along the X and Y directions in the elasticity theory, which assumes that the propagation of stress and strain from a circular loading plate is uniform within a cylindrical coordinate system. Thus, the results verified the validity of the elasticity theory for analyzing loads and

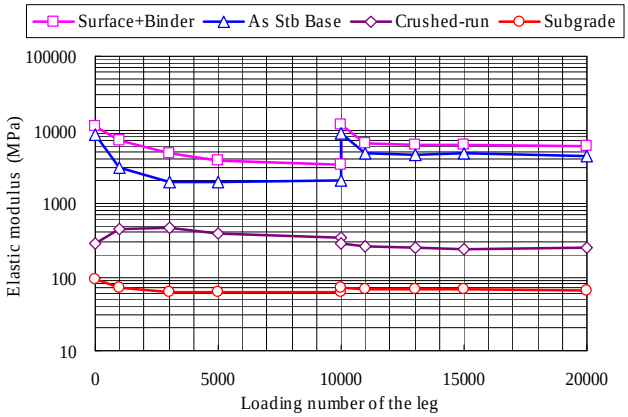

Figure 11 Relation between the estimated elastic modulus and the loading number of gear

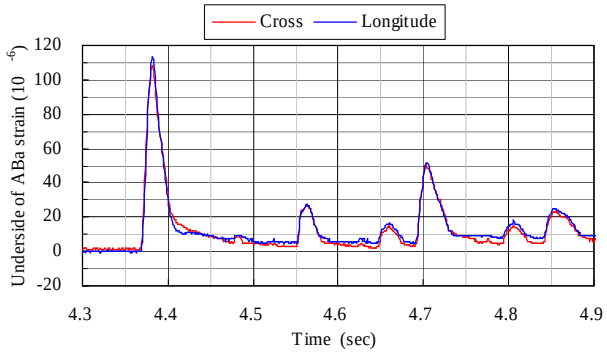

Figure 12 The strain to the longitude direction and the cross direction in the asphalt stabilization underside at the FWD load

deflections measured with FWD.

A comparison between the strain values measured during applied moving gear load and the values calculated using the back-calculated modulus of elasticity is shown in Figure 13. At the underside of the stabilized base, the calculated strain values agreed with the measured strain values at the points where the wheels passed.

On the other hand, under the gear load center, the calculated strain was tensile, while the measured strain was compressive, showing a difference.

The horizontal load at the upperside of the subgrade also showed a similar trend. As pavement is designed by examining the vertical compressive strain, the calculated vertical strain values are shown in Table 1 as well as the calculated and measured horizontal strain values. A comparison between the calculated and measured strain values is shown in Figure 14.

The calculated values agreed well with the measured values under and between the front and rear wheels. However, the calculated strain values were larger than the measured values at the gear center and on the axis of the gear center. The calculations predicted that the vertical strain would be 2.6 times larger than the horizontal strain.

The comparison of the measurement strain which occurred to the asphalt stabilization layer by the movement of the leg load and the calculated strain which was the baccalculated of the elastic modulus is shown in Figure 15. The calculated strain to the longitudinal direction and the cross direction is equal but as for the measurement strain by the moving load, the strain to the longitudinal direction through is bigger than the cross direction. Also, the calculated strain and the measurement strain of the upperside of asphalt stabilized base are similar but the measurement strain of the underside of asphalt stabilized base is quite big than the calculated strain.

Therefore, because of the getting of a dynamic deformation properties and the improvement of the analysis precision, the dynamic analysis will be necessary.

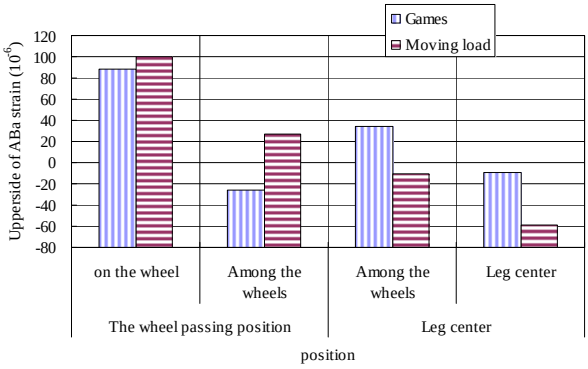

(a) Upperside of the Asphalt Stabilized Base

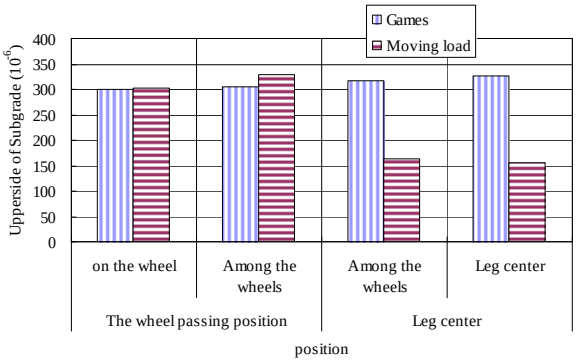

(b) Upperside of the Subgrade

Figure 13 The comparison of the strain at the moving gear load and the strain of the back-calculated modulus

Table 1 The comparison between the measurement strain and the analysis strain of the upperside of subgrade

Static analysis and the moving time (5km/h)		Upperside of Subgrade εr (10^{-6})		εz (10^{-6})
		Analysis	Measurement	Analysis
Plumb down of the wheel	Time of the wheel load	299	303	770
	Center among the wheels	304	329	806
Leg center	On the axle	317	163	827
	Leg center	327	156	880

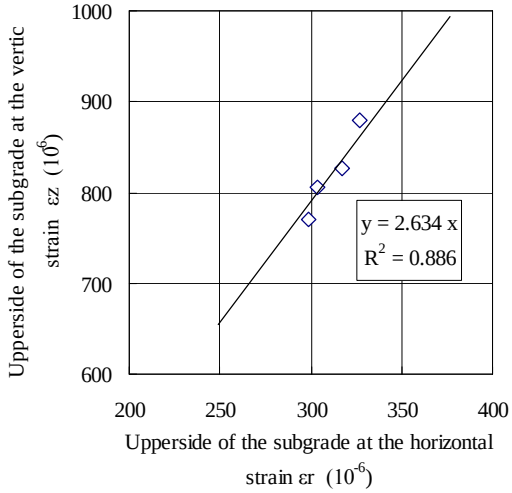

Figure 14 The comparison between the calculated and measured strain values (After 5,000 times)

4.4 Comparison between the results of impact loading test and dynamic analysis

The load and strain measured during applied loads using FWD were analyzed using the software Easy DBALM (Reference 6), which was developed by Prof. Kunihito Matsui of Tokyo Denki University.

A comparison between deflections at 5000 passes measured by FWD and the deflection waveform of DBALM that was back-calculated by dynamic FEM analysis is shown in Figure 16. The moduli of elasticity and attenuation coefficients of the courses, which were determined by the analysis, are shown in Table 2. The measured and analyzed deflection waveforms agreed well with each other. Thus, the calculated moduli of elasticity and the attenuation coefficients per unit area are likely to be reliable.

A comparison between values after 5,000 and 10,000 gear load passes showed that the moduli of elasticity of the asphalt concrete course and the subgrade dropped along with applied loads. The difference in attenuation coefficient between the asphalt concrete course and the stabilized base was 4 MPa.

After 10,000 gear load passes, the attenuation coefficients were similar in the asphalt concrete course and the stabilized base. Deflection increased along with repetitive applied gear load. Decrease in the modulus of elasticity and attenuation coefficient is likely to have been involved in the increase.

The dynamic behavior of runway pavement will be further monitored and investigated to clarify the relationship with fatigue properties.

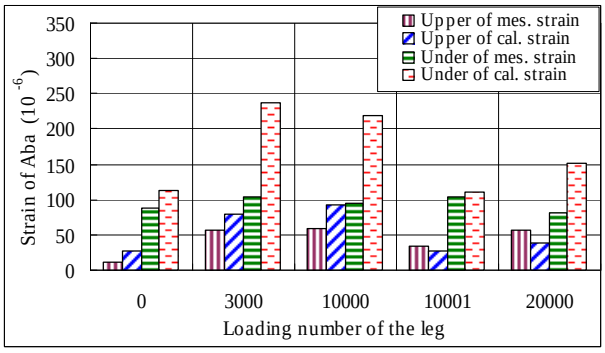

(a) Cross direction

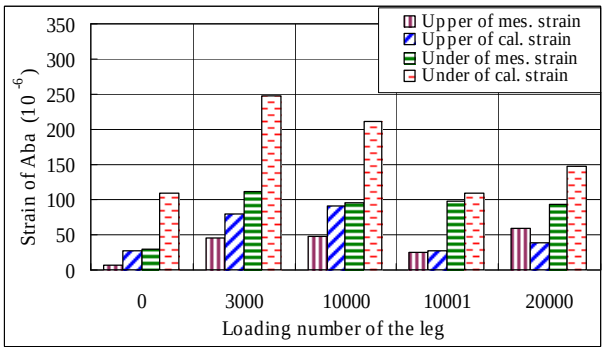

(b) Longitudinal direction

Figure 15 The comparison of the moving strain by the gear load and the strain by the baccalculated elastic modulus

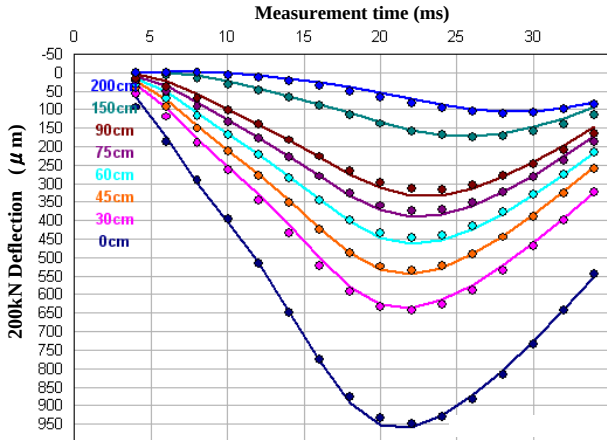

Figure 16 The comparison between deflections at 5000 passes measured by FWD and the deflection waveform of DBALM that was backcalculated by dynamic FEM analysis

Table 2 The elastic modulus and the damping coefficient of each layer which was obtained in this dynamic backcalculation

Pavement	5,000 pass		10,000 pass	
	E (MPa)	D (MPa･s)	E (MPa)	D (MPa･s)
Su+Bi	1216.5	18.63	959.2	16.32
As Stb Base	831.9	14.35	659.0	16.73
C-40	115.2	0.516	148.8	0.569
Subgrade	124.0	0.153	107.8	0.103

5. CONCLUSIONS

Conclusions of this study are summarized below:

1) Tensile strain across the runway was monitored using fiber-optic FBG

sensors embedded in the subgrade and stabilized base.

2) KM strain sensors monitored the strain along the runway as it changed from compressive to tensile strain by the shear force of the gear load.
3) Cutting and overlaying of the surface and binder courses released the static strain of the stabilized base, but repetitive loading increased the residual tensile strain.
4) The tensile strain at the bottom of the stabilized base was 1.3 times larger than that at the top of the stabilized base. The bending fatigue of the pavement caused by loading was critical at the underside of the stabilized base.
5) The strains across and along the runway that were measured during applied load on a circular plate were similar to each other, showing that the elasticity theory can be used to analyze pavement structures.
6) The calculated and measured strains were very similar at the underside of the stabilized base directly under the moving wheels. On the other hand, the calculated strain values at the bottom of the stabilized base and at the top of the subgrade under the gear center were considerably smaller than the strain values measured with KM strain gauges. Dynamic analysis will be conducted by also considering movement along the gear moving direction.
7) The measured strain at the top of the subgrade was largest under the gear center, showing coherence with the principle of superposition of elasticity theory.

ACKNOWLEDGEMENTS

We thank Tokyo Sokki Kenkyujo Co., LTD. and NTT Infra-Net Co., LTD. for their cooperation in selecting strain gauges and conducting measurements of the test pavement. We also thank everyone else involved in this study.

REFERENCES

Maehara, H., Abe, N., Kimura, M., July 2007. *The development of a system to measure the strain on the surface of the pavement caused by the movement of tires*, 6th ICPT, pp. 265–272.

Yuki, T., Abe, N., Manabe, K., Tsubokawa, Y., Ezaki, T., 2007. *Comparison of ground-coupled sensors for the measurement of strain which occurs in airport asphalt pavement*, Japan Society of Civil Engineers (JSCE), 62nd Art and Science Annual Lecture, 5-096, pp. 191–192 (in Japanese).

Fujinami, K., Matsui, K., Nov. 2007. *Development of the static structure analysis software BALM for Windows applied to pavement*, 27th Japan Road Conference, No. 20P08.

Service Center of Port Engineering (SCOPE), April 2005. *Airport civil design, geological survey, soil investigation and inspection common to all application specifications*, (in Japanese).

Maruyama, T., Abe, N., Saika, Y., Himeno, K., Feb. 1994. *Development of structural evaluation and rehabilitation design system for pavement using FWD*, Japan Society of Civil Engineers (JSCE), Collected papers, No. 484, 5-22, pp. 61–68, (in Japanese).

Nishiyama, T., Matsui, K., Kikuta, Y., Higashi, S., 2008. *Development of estimation method for pavement layer densities, damping coefficients and elastic moduli*, JSCE, Collected papers, E category, Vol. 64, No. 4, pp. 572–579, (in Japanese).